

PLANCK 2015 CONSTRAINTS ON THE NON-FLAT XCDM INFLATION MODEL

JUNPEI Ooba,^{1,*} BHARAT RATRA,² AND NAOSHI SUGIYAMA^{1,3,4}

¹*Department of Physics and Astrophysics, Nagoya University, Nagoya 464-8602, Japan*

²*Department of Physics, Kansas State University, 116 Cardwell Hall, Manhattan, KS 66506, USA*

³*Kobayashi-Maskawa Institute for the Origin of Particles and the Universe, Nagoya University, Nagoya, 464-8602, Japan*

⁴*Kavli Institute for the Physics and Mathematics of the Universe (Kavli IPMU), The University of Tokyo, Chiba 277-8582, Japan*

(Dated: October 31, 2018)

ABSTRACT

We examine the Planck 2015 cosmic microwave background (CMB) anisotropy data by using a physically-consistent energy density inhomogeneity power spectrum generated by quantum-mechanical fluctuations during an early epoch of inflation in the non-flat XCDM model. Here dark energy is parameterized using a fluid with a negative equation of state parameter but with the speed of fluid acoustic inhomogeneities set to the speed of light. We find that the Planck 2015 data in conjunction with baryon acoustic oscillation distance measurements are reasonably well fit by a closed XCDM model in which spatial curvature contributes a percent of the current cosmological energy density budget. In this model, the measured non-relativistic matter density parameter and Hubble constant are in good agreement with values determined using most other data. Depending on cosmological parameter values, the closed XCDM model has reduced power, relative to the tilted, spatially-flat Λ CDM case, and can partially alleviate the low multipole CMB temperature anisotropy deficit and can help partially reconcile the CMB anisotropy and weak lensing σ_8 constraints, at the expense of somewhat worsening the fit to higher multipole CMB temperature anisotropy data. However, the closed XCDM inflation model does not seem to improve the agreement much, if at all, compared to the closed Λ CDM inflation case, even though it has one more free parameter.

Keywords: cosmic background radiation — cosmological parameters — large-scale structure of universe
— inflation — observations

* ooba.jiunpei@f.mbox.nagoya-u.ac.jp

1. INTRODUCTION

We recently found that cosmic microwave background (CMB) anisotropy measurements do not require flat spatial hypersurfaces in the Λ CDM scenario (Ooba et al. 2018a; Park & Ratra 2018a,b), provided one uses a physically consistent non-flat model power spectrum of energy density inhomogeneities (Ratra & Peebles 1995; Ratra 2017) in the analysis of the CMB data.

In the standard Λ CDM model (Peebles 1984), dark energy, taken to be the cosmological constant Λ , dominates the current cosmological energy budget and powers the currently accelerating cosmological expansion. Cold dark matter (CDM) is the next largest contributor to the current energy budget, followed by baryonic matter and small contributions from neutrinos and photons. The standard Λ CDM model assumes flat spatial geometry. For reviews of the standard and related scenarios, see Ratra & Vogeley (2008), Martin (2012), Joyce et al. (2016), Huterer & Shafer (2017) and references therein.

It is conventional to parameterize the standard flat- Λ CDM model in terms of six variables: $\Omega_b h^2$ and $\Omega_c h^2$, the current values of the baryonic and cold dark matter density parameters multiplied by the square of the Hubble constant (in units of $100 \text{ km s}^{-1} \text{ Mpc}^{-1}$); θ , the angular diameter distance as a multiple of the sound horizon at recombination; τ , the reionization optical depth; and A_s and n_s , the amplitude and spectral index of the (assumed) power-law primordial scalar energy density inhomogeneity power spectrum, (Planck Collaboration 2016a). The predictions of the flat- Λ CDM model are largely consistent with most available observational constraints (Planck Collaboration 2016a, and references therein).

There are suggestions that flat- Λ CDM might not be as compatible with more recent, larger compilations of measurements (Solà et al. 2017a,b, 2018, 2017c; Zhang et al. 2017) that might be more consistent with dynamical dark energy models. These include the simplest, physically consistent, seven parameter flat- ϕ CDM model in which a scalar field ϕ with potential energy density $V(\phi) \propto \phi^{-\alpha}$ is the dynamical dark energy (Peebles & Ratra 1988; Ratra & Peebles 1988) and $\alpha > 0$ is the seventh parameter and controls dark energy evolution.

Compared to the time-independent Λ , dynamical dark energy density evolves in manner closer to (but slower than) that of spatial curvature energy density. This can cause a complication. Under the assumption of spatial flatness, CMB anisotropy measurements favor Λ although mild dark energy time evolution remains viable. When the general, non-flat, Λ CDM model is used to analyze the CMB data they indicate that spatial hypersurfaces are close to flat although mildly curved space is acceptable. When CMB anisotropy observations are analyzed in a dynamical dark energy model with non-flat spatial hypersurfaces there is degeneracy between spatial curvature and the parameter governing dark energy dynamics. This results in weaker constraints on both parameters, when compared to the cases where only non-zero spatial curvature or only dynamical dark energy is assumed (early references include Aurich & Steiner 2002, 2003, 2004; Crooks et al. 2003; Ichikawa & Takahashi 2006; Wright 2006; Ichikawa et al. 2006; Zhao et al. 2007; Ichikawa & Takahashi 2007; Clarkson et al. 2007; Wang & Mukherjee 2007; Gong et al. 2008; Ichikawa & Takahashi 2008; Hlozek et al. 2008; Virey et al. 2008, and references therein)

Non-zero spatial curvature brings in a new length scale, in addition to the Hubble scale. Consequently in the non-flat case one must use an inflation model to compute a consistent power spectrum. For open spatial hypersurfaces the Gott (1982) open-bubble inflation model is taken as the initial epoch of the cosmological model and one computes zero-point quantum fluctuations during the open inflation epoch and propagates these to the current open, accelerating cosmological expansion epoch where they are energy density inhomogeneities (Ratra & Peebles 1994, 1995).¹ For closed spatial hypersurfaces Hawking's prescription for the quantum state of the universe (Hawking 1984) can be used to construct a closed inflation model (Ratra 1985, 2017). The initial closed inflation epoch linear perturbation solutions constants of integration are determined from closed de Sitter invariant quantum mechanical initial conditions in the Lorentzian section of the closed de Sitter space that follow from Hawking's prescription that the quantum state of the universe only include field configurations regular on the Euclidean (de Sitter) sphere sections (Ratra 1985, 2017). These initial conditions are the unique de Sitter invariant ones. Zero-point quantum-mechanical fluctuations during closed inflation provide a late-time energy density inhomogeneity power spectrum that is not a power law (Ratra 2017); it is a generalization to the closed case (White & Scott 1996; Starobinsky 1996; Zaldarriaga et al. 1998; Lewis et al. 2000; Lesgourgues & Tram 2014) of the flat-space scale-invariant spectrum.

¹ Observational consequences of the open inflation model are discussed in Kamionkowski et al. (1994), Górski et al. (1995), Górski et al. (1998), Ratra et al. (1999), and references therein.

We recently analyzed the Planck 2015 CMB anisotropy data in the non-flat Λ CDM inflation model, using the consistent power spectrum for the non-flat case (Ooba et al. 2018a).² In this paper we examine what constraints these data place on a model in which dark energy is parameterized in terms of a fluid, the so-called XCDM parameterization. Here the dark energy fluid pressure and energy density are related via $p_X = w_0 \rho_X$, where w_0 is the equation of state parameter and is taken to be $< -1/3$. It is well known that such a fluid is unstable and to stabilize it we arbitrarily require that spatial inhomogeneities in the fluid propagate at the speed of light.

Compared to the six parameter flat- Λ CDM inflation model discussed above, in the non-flat case there is no simple tilt option, so n_s is no longer a free parameter and is replaced by the current value of the curvature density parameter Ω_k which results in the six parameter non-flat Λ CDM model (Ooba et al. 2018a). Here we replace the cosmological constant Λ by the dark energy fluid parameterized by w_0 , which is a new free parameter, resulting in the seven parameter non-flat XCDM inflation model.³ Of course, this is not a physical model, and it is also unable to properly mimic the dark energy evolution of the scalar field dynamical dark energy ϕ CDM model (Podariu & Ratra 2001). Nevertheless, it is a simple parameterization of dynamical dark energy that is relatively straightforward to use in a computation and that is worth exploring as a first, and hopefully not misleading, attempt to gain some insight into how dark energy dynamics and non-zero spatial curvature jointly influence the CMB anisotropy data constraints. We note here that there is a physically consistent non-flat seven parameter scalar field dynamical dark energy model (Pavlov et al. 2013); because the scalar field inhomogeneities must be accounted for in this model, the computational demands in ϕ CDM are much more significant than in the XCDM case we study here.

In this paper we use the Planck 2015 CMB anisotropy data to constrain this seven parameter non-flat XCDM inflation model.⁴ We find in this model that the Planck 2015 CMB anisotropy data used jointly with baryon acoustic oscillation (BAO) distance measurements do not require that spatial hypersurfaces be flat. The data favor a slightly closed model. These results are consistent with our earlier analysis of the six parameter non-flat Λ CDM inflation model (Ooba et al. 2018a).

In our analyses here we use different CMB anisotropy data combinations (Planck Collaboration 2016a). For CMB data alone, we find that the best-fit non-flat XCDM model, for the TT + lowP + lensing Planck 2015 data, has spatial curvature density parameter $\Omega_k = -0.021^{+0.023}_{-0.005} {}^{+0.029}_{-0.050}$ (1 and 2σ error bars) and is mildly closed. When we include the BAO data that Planck 2015 used, we find for the TT + lowP + lensing CMB anisotropy case that $\Omega_k = -0.008 \pm 0.003 \pm 0.006$.

As with the six parameter closed- Λ CDM models, it might be significant that the best-fit seven parameter closed XCDM models have less low ℓ CMB temperature anisotropy C_ℓ power than does the best-fit six parameter tilted, spatially-flat Λ CDM model, and so appear to be in slightly better agreement with the low- ℓ temperature C_ℓ observations (less so when the BAO data are included in the analysis). Overall, however, the best-fit seven parameter closed XCDM inflation model does not do better, and probably does a little worse, than the best-fit six parameter closed Λ CDM inflation model we studied earlier (Ooba et al. 2018a).

In Sec. II we summarize the methods we use. Our parameter constraints are plotted, tabulated, and discussed in Sec. III, where we also attempt to determine how well the best-fit closed-XCDM case fits the data. Conclusions are given in Sec. IV.

2. METHODS

For our non-flat model analyses we use the open and closed inflation model energy density inhomogeneity power spectrum (Ratra & Peebles 1995; Ratra 2017). Figure 1 compares closed XCDM and Λ CDM inflation model power spectra and a tilted flat- Λ CDM inflation model power spectrum. We use the public numerical code CLASS (Blas et al. 2011) to compute the angular power spectra of the CMB temperature, polarization, and lensing potential anisotropies. Our parameter estimations are carried out using the Markov chain Monte Carlo method program Monte Python (Audren et al. 2013).

We assume flat priors for the cosmological parameters over the ranges

$$\begin{aligned} 100\theta &\in (0.5, 10), \quad \Omega_b h^2 \in (0.005, 0.04), \quad \Omega_c h^2 \in (0.01, 0.5), \\ \tau &\in (0.005, 0.5), \quad \ln(10^{10} A_s) \in (0.5, 10), \quad \Omega_k \in (-0.5, 0.5), \quad w_0 \in (-3, 0.2). \end{aligned} \quad (1)$$

² A similar analysis, with similar conclusions, has been carried out for the non-flat ϕ CDM inflation model (Ooba et al. 2018b; Park & Ratra 2018c).

³ We study the seven parameter flat XCDM inflation model elsewhere (Ooba et al. 2018c).

⁴ Zhao et al. (2017) and Di Valentino et al. (2017) have recently studied other variants of flat XCDM designed to resolve cosmological tensions.

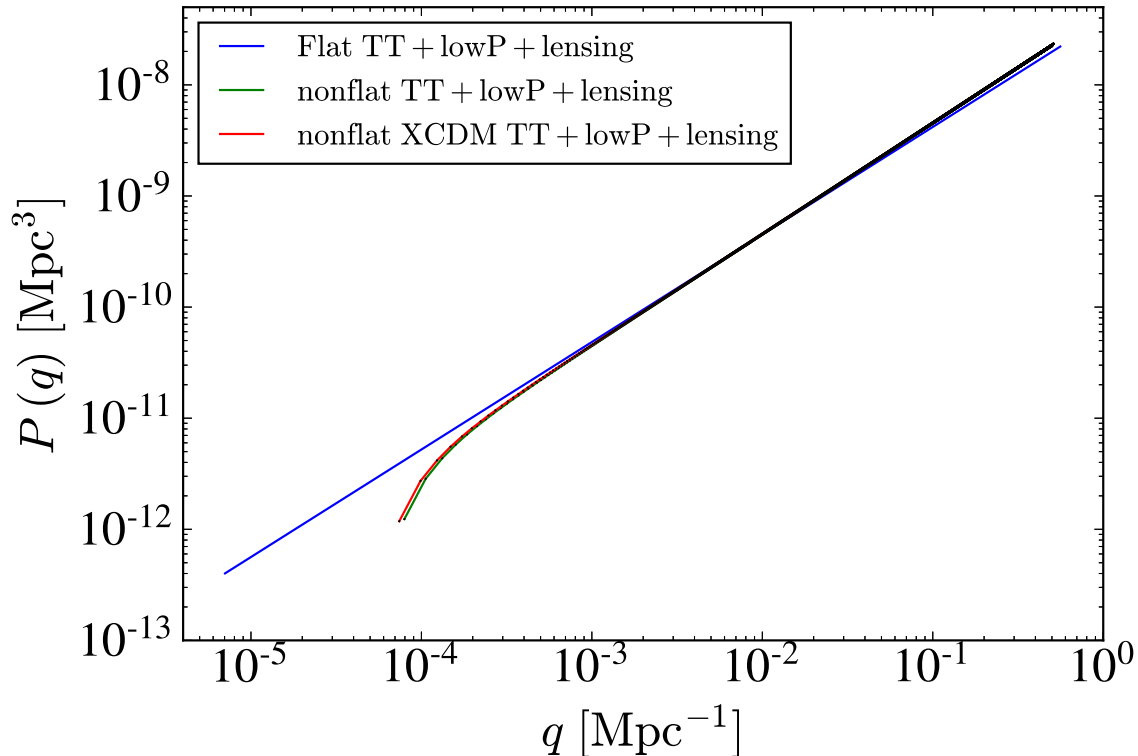


Figure 1. Best-fit (see text) gauge-invariant fractional energy density inhomogeneity power spectra. The blue line corresponds to the tilted flat- Λ CDM model of [Planck Collaboration \(2016a\)](#). In the closed case, wavenumber $q \propto A + 1$ where the eigenvalue of the spatial Laplacian is $-A(A + 2)$, A is a non-negative integer, $A = 0$ corresponds to the constant zero-mode on the three sphere, the power spectrum vanishes at $A = 1$, and the points on the red and green curves correspond to $A = 2, 3, 4, \dots$, see eqns. (8) and (203) of [Ratra \(2017\)](#). On large scales the power spectra for the best-fit closed XCDM (red curve) and Λ CDM (green curve) models are suppressed relative to that of the best-fit tilted flat- Λ CDM model. The $P(q)$ are normalized using the best-fit values of A_s at the pivot scale $k_0 = 0.05$ [Mpc^{-1}].

The CMB temperature and the effective number of neutrinos are taken to be $T_{\text{CMB}} = 2.7255$ K from COBE ([Fixsen 2009](#)) and $N_{\text{eff}} = 3.046$ with one massive (0.06 eV) and two massless neutrino species in a normal hierarchy. The primordial helium fraction Y_{He} is inferred from standard Big Bang nucleosynthesis as a function of the baryon density.

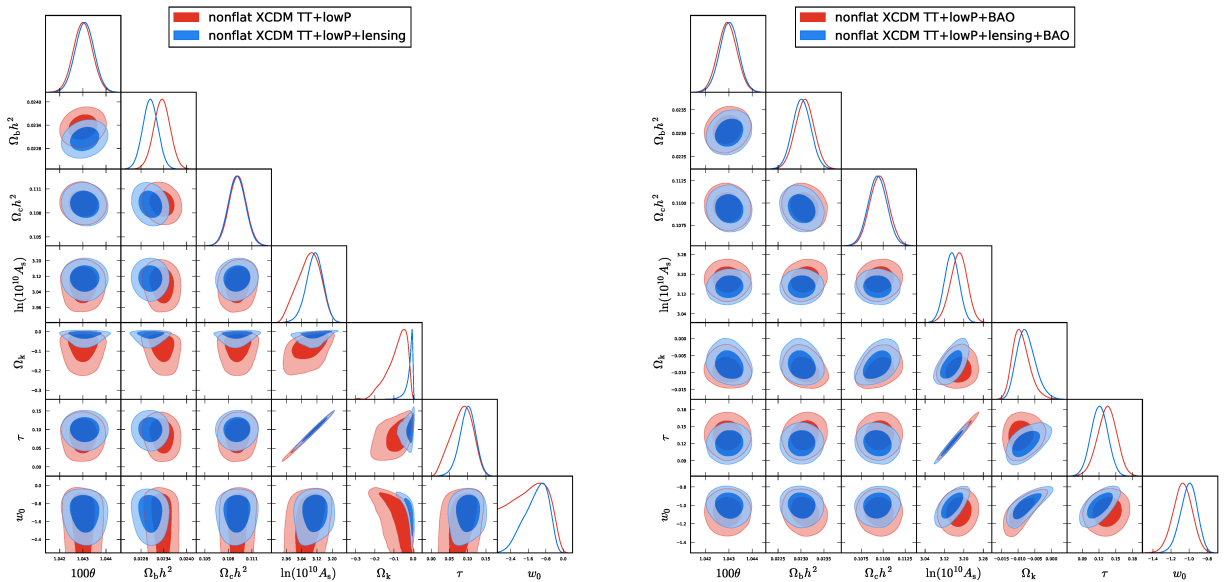
We constrain model parameters by comparing model predictions to the CMB angular power spectrum data from the Planck 2015 mission ([Planck Collaboration 2016a](#)) and the BAO distance measurements of the 6dF Galaxy Survey ([Beutler et al. 2011](#)), the Baryon Oscillation Spectroscopic Survey (LOWZ and CMASS) ([Anderson et al. 2014](#)), and the Sloan Digital Sky Survey main galaxy sample (MGS) ([Ross et al. 2015](#)).

3. RESULTS

In this section we present results of our parameter estimation computations and our attempt to determine how well the best-fit seven parameter closed-XCDM inflation case does relative to the best-fit six parameter tilted flat- Λ CDM inflation model ([Planck Collaboration 2016a](#)) and the best-fit six parameter closed- Λ CDM inflation model ([Ooba et al. 2018a](#)). Table 1 lists central values and 68.27% (1σ) limits on the cosmological parameters from the various CMB and BAO data sets we use. Figure 2 shows two-dimensional constraint contour and one-dimensional likelihood (determined by marginalizing over all other parameters) plots, derived from the two CMB anisotropy data sets, both excluding and including the BAO data. Figure 3 plots the CMB temperature anisotropy angular power spectra for the best-fit non-flat XCDM cases determined from the two different CMB anisotropy data sets (as well as for the non-flat and tilted spatially-flat Λ CDM models), excluding and including the BAO data, Figure 4 shows 68.27% and 95.45% (2σ) confidence contours in the σ_8 - Ω_m plane, after marginalizing over the other parameters, for the non-flat XCDM inflation cases as well as for one spatially-flat tilted Λ CDM inflation model, without and with the BAO data.

Table 1. 68.27% confidence limits on cosmological parameters of the non-flat XCDM model from CMB and BAO data.

Parameter	TT+lowP	TT+lowP+lensing	TT+lowP+BAO	TT+lowP+lensing+BAO
$\Omega_b h^2$	0.02335 ± 0.00022	0.02304 ± 0.00021	0.02308 ± 0.00021	0.02301 ± 0.00020
$\Omega_c h^2$	0.1092 ± 0.0011	0.1091 ± 0.0011	0.1096 ± 0.0011	0.1094 ± 0.0011
100θ	1.04301 ± 0.00042	1.04307 ± 0.00041	1.04294 ± 0.00042	1.04301 ± 0.00041
τ	0.084 ± 0.031	0.100 ± 0.022	0.134 ± 0.017	0.121 ± 0.015
$\ln(10^{10} A_s)$	3.077 ± 0.062	3.107 ± 0.044	3.178 ± 0.035	3.150 ± 0.030
Ω_k	-0.086 ± 0.048	-0.021 ± 0.014	-0.009 ± 0.003	-0.008 ± 0.003
w_0	-1.55 ± 0.86	-1.23 ± 0.56	-1.07 ± 0.11	-1.00 ± 0.10
H_0 [km/s/Mpc]	55.53 ± 12.76	73.96 ± 20.29	69.52 ± 2.16	68.36 ± 1.93
Ω_m	0.52 ± 0.24	0.31 ± 0.14	0.28 ± 0.02	0.28 ± 0.02
σ_8	0.829 ± 0.134	0.865 ± 0.162	0.852 ± 0.034	0.820 ± 0.022
$S_8 \equiv \sigma_8 \sqrt{\Omega_m/0.3}$	1.020 ± 0.104	0.795 ± 0.084	0.815 ± 0.019	0.797 ± 0.012

**Figure 2.** 68.27% and 95.45% confidence level contours for the non-flat XCDM inflation model using various data sets, with the other parameters marginalized.

From the analysis without the BAO data, the spatial curvature density parameter is measured to be

$$\Omega_k = -0.021^{+0.029}_{-0.050} \quad (95.45\%, \text{ TT + lowP + lensing}). \quad (2)$$

The left hand panels of Fig. 3 show the CMB temperature anisotropy C_ℓ of the best-fit non-flat XCDM inflation cases for the 2 different CMB data sets. It appears that these models fit the low- ℓ C_ℓ observations better than does the spatially-flat tilted Λ CDM case of [Planck Collaboration \(2016a\)](#), with the higher- ℓ C_ℓ data not as well fit by the non-flat models. On large scales the fractional energy density inhomogeneity power spectrum for the best-fit closed XCDM and Λ CDM inflation models are suppressed relative to that of the best-fit tilted flat- Λ CDM model, as shown in Fig. 1 for the TT + lowP + lensing data. The low- ℓ C_ℓ of Fig. 3 depend on this small wavenumber part of the power spectrum, but other effects, such as the usual and integrated Sachs-Wolfe effects, also play an important role in determining the C_ℓ shape. The left panel of Fig. 4 shows σ_8 - Ω_m constraint contours for the 2 non-flat XCDM cases (as well as for one spatially-flat tilted Λ CDM model). With CMB lensing included, we find that our non-flat

seven parameter Λ CDM inflation model reduces the tension between the CMB observations and the weak lensing data, compare Fig. 4 here to Fig. 18 of [Planck Collaboration \(2016a\)](#).⁵

From the analysis also including the BAO data, the spatial curvature density parameter is measured to be

$$\Omega_k = -0.008 \pm 0.006 \quad (95.45\%, \text{ TT} + \text{lowP} + \text{lensing} + \text{BAO}). \quad (3)$$

In contrast to the Planck 2015 results ([Planck Collaboration 2016a](#)), our physically-consistent non-flat Λ CDM inflation model is not forced to be flat even with the BAO data included in the analysis. This case is about 3σ away from flat. The right panels of Fig. 3 show temperature C_ℓ plots for the best-fit non-flat Λ CDM models analyzed using the 2 different CMB data sets and including the BAO data. Including the BAO data does somewhat degrade the fit in the low- ℓ region compared with results from the analyses without the BAO data. We find that including the BAO data also worsens the σ_8 - Ω_m plane tension between the CMB and weak lensing constraints, see the right hand panel of Fig. 4.

It is interesting that the Ω_m and H_0 constraints listed in Table 1 are very consistent with estimates for these parameters from most other data. See [Chen & Ratra \(2003\)](#) for the density parameter. The most recent median statistics analysis of H_0 measurements gives $H_0 = 68 \pm 2.8 \text{ km s}^{-1} \text{ Mpc}^{-1}$ ([Chen & Ratra 2011](#)), consistent with earlier estimates ([Gott et al. 2001](#); [Chen et al. 2003](#)). Many recent H_0 determinations from BAO, Type Ia supernovae, Hubble parameter, and other measurements are consistent with these results ([Calabrese et al. 2012](#); [Hinshaw et al. 2013](#); [Sievers et al. 2013](#); [Aubourg et al. 2015](#); [L’Huillier & Shafieloo 2017](#); [Luković et al. 2016](#); [Chen et al. 2017](#); [Wang et al. 2017](#); [Lin & Ishak 2017](#)). It is however well known that local measurements of the expansion rate find a higher H_0 value. [Freedman et al. \(2012\)](#) give $H_0 = 74.3 \pm 2.1 \text{ km s}^{-1} \text{ Mpc}^{-1}$ while [Riess et al. \(2016\)](#) report $H_0 = 73.24 \pm 1.74 \text{ km s}^{-1} \text{ Mpc}^{-1}$, somewhat higher than the $H_0 = 68.36 \pm 1.93 \text{ km s}^{-1} \text{ Mpc}^{-1}$ of the last column of Table 1.

In addition, we note that many analyses based on a number of different observations also do not rule out non-flat dark energy models ([Farooq et al. 2015](#); [Sapone et al. 2014](#); [Li et al. 2014](#); [Cai et al. 2016](#); [Chen et al. 2016](#); [Yu & Wang 2016](#); [L’Huillier & Shafieloo 2017](#); [Farooq et al. 2017](#); [Li et al. 2016](#); [Wei & Wu 2017](#); [Rana et al. 2017](#); [Yu et al. 2018](#); [Mitra et al. 2018](#); [Ryan et al. 2018](#)).

Table 2. Minimum χ^2 values for the best-fit closed- Λ CDM (and tilted flat- Λ CDM) inflation model.

Data sets	χ^2	d.o.f.
TT+lowP	11277 (11262)	188 (189)
TT+lowP+lensing	11292 (11272)	196 (197)
TT+lowP+BAO	11289 (11266)	192 (193)
TT+lowP+lensing+BAO	11298 (11277)	200 (201)

Table 3. χ^2 values for the best-fit closed- Λ CDM (and tilted flat- Λ CDM) inflation model.

Data	TT+lowP	TT+lowP+lensing	TT+lowP+BAO	TT+lowP+lensing+BAO
CMB low- ℓ	130.15 (129.83)	131.39 (126.06)	140.07 (130.06)	129.78 (126.00)
CMB high- ℓ	138.86 (77.13)	121.31 (82.46)	143.45 (73.64)	134.92 (80.82)
CMB all- ℓ	269.01 (206.97)	262.99 (218.43)	286.44 (207.73)	279.18 (220.31)
CMB lensing	—	9.81 (9.90)	—	9.77 (9.92)
BAO	—	—	2.92 (4.03)	4.70 (3.58)
d.o.f.	188 (189)	196 (197)	192 (193)	200 (201)

⁵ Note that, as discussed in Sec. 5 of [Planck Collaboration \(2016a\)](#), because of the incorrect amount of lensing in the TT power spectrum, this tension is also alleviated when the Planck lensing reconstruction data is used ([Renzi et al. 2018](#)). For another option see [Di Valentino et al. \(2018\)](#).

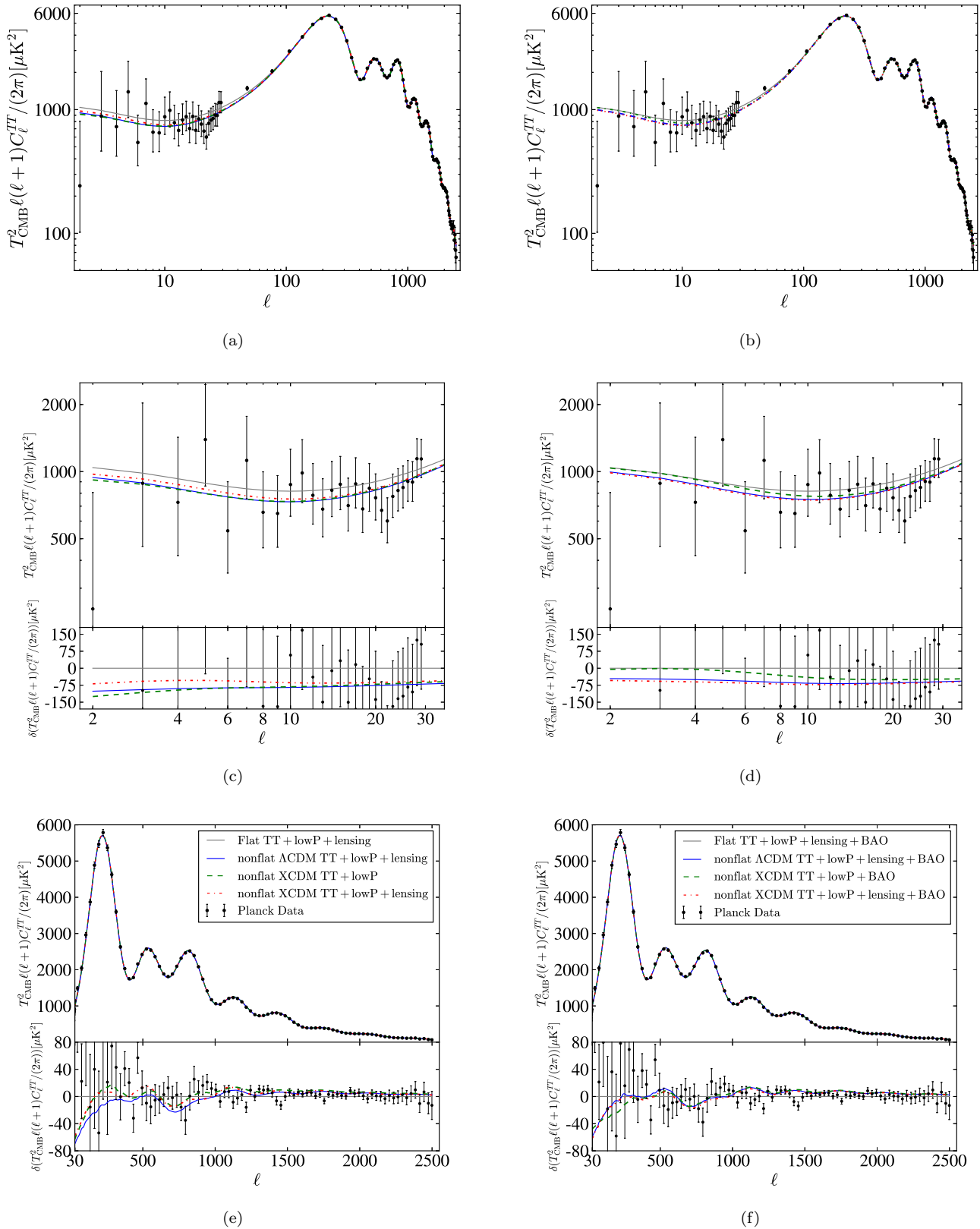


Figure 3. Temperature C_ℓ for the best-fit non-flat XCDM, non-flat Λ CDM and spatially-flat tilted Λ CDM (gray solid line) models. Linestyle information are listed in the boxes in the two bottom panels. Planck 2015 measurements are shown as black points with error bars. Left panels (a), (c) and (e) are from CMB data alone analyses, while right panels (b), (d) and (f) analyses also include BAO data. Top panels show the all- ℓ region. Middle panels show the low- ℓ region C_ℓ and residuals. Bottom panels show the high- ℓ region C_ℓ and residuals.

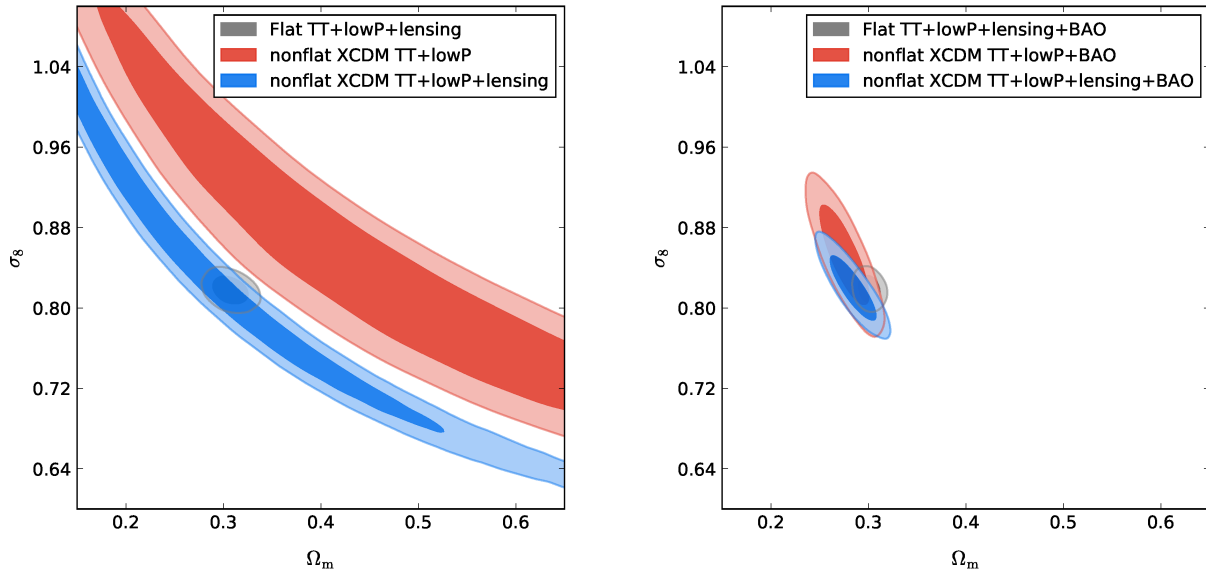


Figure 4. 68.27% and 95.45% confidence contours in the σ_8 - Ω_m plane. Left panel shows Planck data alone contours while right panel contours also account for BAO data.

It is vital to understand how well the best-fit closed-XCDM inflation case does relative to the best-fit tilted flat- Λ CDM model in fitting the data. As for the closed- Λ CDM model (Ooba et al. 2018a), we are unable to resolve this in a quantitative manner, although qualitatively, overall, the best-fit closed-XCDM model does not do as well as the best-fit tilted flat- Λ CDM model. It also appears to not do as well as the best-fit closed- Λ CDM inflation model (Ooba et al. 2018a), which has one fewer parameter.

Table 2 lists the minimum $\chi^2 = -2\ln(L_{\max})$ determined from the maximum value of the likelihood, for the 4 data sets we consider, for both the closed-XCDM and tilted flat- Λ CDM inflation models, as well as the number of (binned data) degrees of freedom (d.o.f.). The d.o.f. are determined from combinations of 112 low- ℓ TT + lowP, 83 high- ℓ TT, 8 lensing CMB (binned) measurements, 4 BAO observations, and 7 (or 6 for the tilted flat- Λ CDM) model parameters. It is likely that the large χ^2 values are the result of the many nuisance parameters that have been marginalized over, since the tilted flat- Λ CDM model is said to be a good fit to the data. From this table we see that $\Delta\chi^2 = 20(21)$ for the closed-XCDM inflation case (196 (200) d.o.f.), relative to the tilted flat- Λ CDM (197 (201) d.o.f.), for the TT + low P + lensing (+ BAO) data. This might make the closed-XCDM case much less probable, however, one can see from the residual panels of Fig. 3 (e) & (f) that this $\Delta\chi^2$ appears to be a consequences of many small deviations, and not of a few significant outliers.

Though there are correlations in the data, it is useful to also consider a standard goodness of fit χ^2 that makes use of only the diagonal elements of the correlation matrix. These χ^2 's are listed in Table 3 for the 4 data sets we study and for both the closed-XCDM and tilted flat- Λ CDM inflation models. From Table 3 for the TT + low P + lensing data, the χ^2 per d.o.f. is 273/196 (227/197) for the closed-XCDM (tilted flat- Λ CDM) inflation model, and when BAO data is included these become 294/200 (234/201). Again, while the closed-XCDM case is less favored than the tilted flat- Λ CDM case, it is not clear how to assess the quantitative significance of this. In addition to the discussion at the end of the previous paragraph, here we have also ignored all off-diagonal information in the correlation matrix, so it is meaningless to compute standard probabilities from such χ^2 's. In summary, while the best-fit closed-XCDM inflation case appears less favored, it might be useful to perform a more thorough analysis of the model.

We additionally compute the Bayesian evidence for each of the models we consider, by using the public numerical code MCEvidence (Heavens et al. 2017). We then compute the natural logarithm of the ratio of the Bayesian evidence of our model to that of the spatially-flat tilted Λ CDM model, which we write as $\ln(B)$. For the TT + low P (+ lensing) case, we get $\ln(B) = +4.08 (-3.79)$, and for the TT + low P + BAO (+ lensing) case, we find $\ln(B) = -14.98 (-18.51)$. According to Kass & Raftery (1995), $|\ln B| > 3$ is strong evidence and $|\ln B| > 5$ is very strong. So our model is favored when we use the TT + low P data, while it is less favored than tilted flat- Λ CDM when we consider the other data sets.

4. CONCLUSION

We determine Planck 2015 CMB data constraints on the physically consistent seven parameter non-flat XCDM model with inflation-generated energy density inhomogeneity power spectrum. This is a first attempt to examine the effect of the interplay between dark energy dynamics and spatial curvatures on constraints derived from CMB anisotropy measurements. We again draw attention to the fact that the X-fluid dark energy part of the XCDM model is only a parameterization, and not a physical model, and hope it does not lead to misleading conclusions.

Unlike the case for the seven parameter non-flat tilted Λ CDM model with the physically-inconsistent power spectrum used in [Planck Collaboration \(2016a\)](#), we discover that CMB anisotropy data do not force spatial curvature to vanish in our non-flat XCDM inflation model with a physically-consistent power spectrum. This is consistent with what we found in the six parameter non-flat Λ CDM inflation model ([Ooba et al. 2018a](#)), where spatial curvature contributes about 2 % to the present energy budget of the closed model that best fits the Planck TT + lowP + lensing data. These closed inflation models are more consistent with the low- ℓ C_ℓ temperature observations and the weak lensing σ_8 measurements than is the best fit spatially-flat tilted Λ CDM, but they do worse at fitting the higher- ℓ C_ℓ data.⁶

It might be useful to reexamine the issue of possible small differences in cosmological parameter constraints derived from higher- ℓ and from lower- ℓ Planck 2015 CMB anisotropy data ([Addison et al. 2016](#); [Planck Collaboration 2016b](#)), by using the non-flat XCDM model. In addition we note that in the tilted flat Λ CDM model there seem to be inconsistencies between the higher- ℓ Planck and the South Pole Telescope CMB data ([Aylor et al. 2017](#)). Also of great interest would be a method for quantitatively assessing how well the best-fit tilted spatially-flat Λ CDM model and the best-fit non-flat XCDM case fit the Planck 2015 CMB anisotropy (and other cosmological) measurements.

Unlike the analysis for the seven parameter non-flat tilted Λ CDM model in [Planck Collaboration \(2016a\)](#), also including the BAO data in the mix does not force our seven parameter non-flat XCDM case to be flat; in fact, $\Omega_k = -0.008 \pm 0.006$ at 2σ and is about 3σ away from flat. In this case the improved agreement with the low- ℓ C_ℓ temperature data and the weak lensing σ_8 constraints are not as good compared with the results from the analyses using only the CMB observations. We note that the BAO and CMB data are from very different redshifts and it is possible that a better model for the intervening epoch or an improved understanding of one or both sets of observations might alter this finding.

Perhaps adding a small spatial curvature contribution, of order a percent, can improve the spatially-flat standard Λ CDM model. However, it appears that the six parameter closed- Λ CDM inflation model might do a better job at this ([Ooba et al. 2018a](#); [Park & Ratra 2018a,b](#)) than does the seven parameter closed-XCDM inflation model we studied here. A more thorough analysis of the non-flat Λ CDM and XCDM inflation models is needed to establish if either is viable and can help resolve some of the low- ℓ C_ℓ issues as well as possibly the σ_8 power issues. Perhaps non-zero spatial curvature might be more important for this purpose than is dark energy dynamics.

ACKNOWLEDGMENTS

WE acknowledge valuable discussions with C.-G. Park. This work is supported by Grants-in-Aid for Scientific Research from JSPS (Nos. 16J05446 (J.O.) and 15H05890 (N.S.)). B.R. is supported in part by DOE grant DE-SC0019038.

⁶ Deuterium abundance measurements mildly favor the flat case over the open one ([Penton et al. 2018](#)) while a compilation of all recent BAO, Type Ia supernova, and Hubble parameter data mildly favor closed spatial hypersurfaces ([Park & Ratra 2018d](#)).

REFERENCES

- Addison, G. E., et al. 2016, *ApJ*, 818, 132 [arXiv:1511.00055]
- Anderson, L. et al. 2014, *MNRAS*, 441, 24 [arXiv:1312.4877]
- Aubourg, É. et al. 2015, *Phys. Rev. D*, 92, 123516 [arXiv:1411.1074]
- Audren, B., Lesgourgues, J., Benabed, K., & Prunet, S. 2013, *JCAP*, 1302, 001 [arXiv:1210.7183]
- Aurich, R., & Steiner, F. 2002, *MNRAS*, 334, 735 [arXiv:astro-ph/0109288]
- Aurich, R., & Steiner, F. 2003, *Phys. Rev. D*, 67, 123511 [arXiv:astro-ph/0212471]
- Aurich, R., & Steiner, F. 2004, *Int. J. Mod. Phys. D*, 13, 123 [arXiv:astro-ph/0302264]
- Aylor, K., Hou, Z., Knox, L., et al. 2017, *ApJ*, 850, 101 [arXiv:1706.10286]
- Beutler, F. et al. 2011, *MNRAS*, 416, 3017 [arXiv:1106.3366]
- Blas, D., Lesgourgues, J., & Tram, T. 2011, *JCAP*, 1107, 034 [arXiv:1104.2933]
- Cai, R.-G., Guo, Z.-K., & Yang, T. 2016, *Phys. Rev. D*, 93, 043517 [arXiv:1509.06283]
- Calabrese, E., Archidiacono, M., Melchiorri, A., & Ratra, B. 2012, *Phys. Rev. D*, 86, 043520 [arXiv:1205.6753]
- Chen, G., Gott, J. R., & Ratra, B. 2003, *PASP*, 115, 1269 [arXiv:astro-ph/0308099]
- Chen, G., & Ratra, B. 2003, *PASP*, 115, 1143 [arXiv:astro-ph/0302002]
- Chen, G., & Ratra, B. 2011, *PASP*, 123, 1127 [arXiv:1105.5206]
- Chen, Y., Kumar, S., & Ratra, B. 2017, *ApJ*, 835, 86 [arXiv:1606.07316]
- Chen, Y., et al. 2016, *ApJ*, 829, 61 [arXiv:1603.07115]
- Clarkson, C., Cortès, M., & Bassett, B. 2007, *JCAP*, 0708, 011 [arXiv:astro-ph/0702670]
- Crooks, J. L., et al. 2003, *Astropart. Phys.*, 20, 361 [arXiv:astro-ph/0305495]
- Di Valentino, E., Bøehm, C., Hivon, E., & Bouchet, F. R. 2018, *PhRvD*, 97, 043513 [arXiv:1710.02519]
- Di Valentino, E., Melchiorri, A., Linder, E. V., & Silk, J. 2017, *PhRvD*, 96, 023523 [arXiv:1704.00762]
- Farooq, O., Madiyar, F. R., Crandall, S., & Ratra, B. 2017, *ApJ*, 835, 26 [arXiv:1607.03537]
- Farooq, O., Mania, D., & Ratra, B. 2015, *ApSS*, 357, 11 [arXiv:1308.0834]
- Fixsen, D. J. 2009, *ApJ*, 707, 916 [arXiv:0911.1955]
- Freedman, W. L., et al. 2012, *ApJ*, 758, 24 [arXiv:1208.3281]
- Gong, Y., Wu, Q., & Wang, A. 2008, *ApJ*, 681, 27 [arXiv:0708.1817]
- Górski, K. M., et al. 1998, *ApJS*, 114, 1 [arXiv:astro-ph/9608054]
- Górski, K. M., Ratra, B., Sugiyama, N., & Banday, A. J. 1995, *ApJ*, 444, L65 [arXiv:astro-ph/9502034]
- Gott, J. R. 1982, *Nature*, 295, 304
- Gott, J. R., Vogeley, M. S., Podariu, S., & Ratra, B. 2001, *ApJ*, 549, 1 [arXiv:astro-ph/0006103]
- Hawking, S. W. 1984, *Nucl. Phys. B*, 239, 257
- Heavens, A., Fantaye, Y., Mootoovaloo, A., et al. 2017, arXiv:1704.03472
- Hinshaw, G., et al. 2013, *ApJS*, 208, 19 [arXiv:1212.5226]
- Hlozek, R., Cortès, M., Clarkson, C., & Bassett, B. 2008, *Gen. Relativ. Gravit.*, 40, 285 [arXiv:0801.3847]
- Huterer, D., & Shafer, D. L. 2017, arXiv:1709.01091
- Ichikawa, K., Kawasaki, M., Sekiguchi, T., & Takahashi, T. 2006, *JCAP*, 0612, 005 [arXiv:astro-ph/0605481]
- Ichikawa, K., & Takahashi, T. 2006, *Phys. Rev. D*, 73, 083526 [arXiv:astro-ph/0511821]
- Ichikawa, K., & Takahashi, T. 2007, *JCAP*, 0702, 001 [arXiv:astro-ph/0612739]
- Ichikawa, K., & Takahashi, T. 2008, *JCAP*, 0804, 027 [arXiv:0710.3995]
- Joyce, A., Lombriser, L., & Schmidt, F. 2016, *Ann. Rev. Nucl. Part. Sci.*, 66, 95 [arXiv:1601.06133]
- Kamionkowski, M., Ratra, B., Spergel, D. N., & Sugiyama, N. 1994, *ApJ*, 434, L1 [arXiv:astro-ph/9406069]
- Kass, R. E., & Raftery, A. E. 1995, *Journal of the American Statistical Association*, 90, 773
- Lesgourgues, J., & Tram, T. 2014, *JCAP*, 1409, 032 [arXiv:1312.2697]
- Lewis, A., Challinor, A., & Lasenby, A. 2000, *ApJ*, 538, 473 [arXiv:astro-ph/9911177]
- L’Huillier, B., & Shafieloo, A. 2017, *JCAP*, 1701, 015 [arXiv:1606.06832]
- Li, Y.-L., Li, S.-Y., Zhang, T.-J., & Li, T.-P. 2014, *ApJ*, 789, L15 [arXiv:1404.0773]
- Li, Z., Wang, G.-J., Liao, K., & Zhu, Z.-H. 2016, *ApJ*, 833, 240 [arXiv:1611.00359]
- Lin, W., & Ishak, M. 2017, *PhRvD*, 96, 083532 [arXiv:1708.09813]
- Luković, V. V., D’Agostino, R., & Vittorio, N. 2016, *Astron. Astrophys.*, 595, A109 [arXiv:1607.05677]
- Martin, J., 2012, *C. R. Physique*, 13, 566 [arXiv:1205.3365]
- Mitra, S., Choudhury, T. R., & Ratra, B. 2018, *MNRAS*, 479, 4566 [arXiv:1712.00018]
- Ooba, J., Ratra, B., & Sugiyama, N. 2018a, *ApJ*, 864, 80 [arXiv:1707.03452]
- Ooba, J., Ratra, B., & Sugiyama, N. 2018b, *ApJ*, 866, 68 [arXiv:1712.08617]

- Ooba, J., Ratra, B., & Sugiyama, N. 2018c, arXiv:1802.05571
- Park, C.-G., & Ratra, B. 2018a, ApJ, in press [arXiv:1801.00213]
- Park, C.-G., & Ratra, B. 2018b, arXiv:1803.05522
- Park, C.-G., & Ratra, B. 2018c, arXiv:1807.07421
- Park, C.-G., & Ratra, B. 2018d, arXiv:1809.03598
- Pavlov, A., Westmoreland, S., Saaidi, K., & Ratra, B. 2013, Phys. Rev. D, 88, 123513 [arXiv:1307.7399]
- Peebles, P. J. E. 1984, ApJ, 284, 439
- Peebles, P. J. E., & Ratra, B. 1988, ApJ, 325, L17
- Penton, J., Peyton, J., Zahoor, A., & Ratra, B. 2018, PASP, 130, 114001 [arXiv:1808.01490]
- Planck Collaboration 2016a, Astron. Astrophys., 594, A13 [arXiv:1502.01589]
- Planck Collaboration 2016b, arXiv:1608.02487
- Podariu, S., & Ratra, B. 2001, ApJ, 532, 109 [arXiv:astro-ph/9910527]
- Rana, A., Jain, D., Mahajan, S., & Mukherjee, A. 2017, JCAP, 1703, 028 [arXiv:1611.07196]
- Ratra, B. 1985, Phys. Rev. D, 31, 1931
- Ratra, B. 2017, PhRvD, 96, 103534 [arXiv:1707.03439]
- Ratra, B., & Peebles, P. J. E. 1988, Phys. Rev. D, 37, 3406
- Ratra, B., & Peebles, P. J. E. 1994, ApJ, 432, L5
- Ratra, B., & Peebles, P. J. E. 1995, Phys. Rev. D, 52, 1837
- Ratra, B., et al. 1999, ApJ, 517, 549 [arXiv:astro-ph/9901014]
- Ratra, B., & Vogeley, M. 2008, PASP, 120, 235 [arXiv:0706.1565]
- Renzi, F., Di Valentino, E., & Melchiorri, A. 2018, PhRvD, 97, 123534 [arXiv:1712.08758]
- Riess, A. G., et al. 2016, ApJ, 826, 56 [arXiv:1604.01424]
- Ross, A. J. et al. 2015, MNRAS, 449, 835 [arXiv:1409.3242]
- Ryan, J., Doshi, S., & Ratra, B. 2018, MNRAS, 480, 759 [arXiv:1805.06408]
- Sapone, D., Majerotto, E., & Nesseris, S. 2014, Phys. Rev. D, 90, 023012 [arXiv:1402.2236]
- Sievers, J. L., et al. 2013, JCAP, 1310, 060 [arXiv:1301.0824]
- Solà, J., de Cruz Pérez, J., & Gómez-Valent, A. 2018, Europhys. Lett., 121, 39001 [arXiv:1606.00450]
- Solà, J., de Cruz Pérez, J. & Gómez-Valent, A. 2017c, arXiv:1703.08218
- Solà, J., Gómez-Valent, A., & de Cruz Pérez, J. 2017a, ApJ, 836, 43 [arXiv:1602.02103]
- Solà, J., Gómez-Valent, A., & de Cruz Pérez, J. 2017b, Mod. Phys. Lett. A, 32, 1750054 [arXiv:1610.08965]
- Starobinsky, A. A. 1996, arXiv:astro-ph/9603075
- Virey, J.-M., et al. 2008, JCAP, 0812, 008 [arXiv:0802.4407]
- Wang, Y., & Mukherjee, P. 2007, Phys. Rev. D, 76, 103533 [arXiv:astro-ph/0703780]
- Wang, Y., Xu, L., & Zhao, G.-B. 2017, arXiv:1706.09149
- Wei, J.-J., & Wu, X.-F. 2017, ApJ, 838, 160 [arXiv:1611.00904]
- White, M., & Scott, D. 1996, ApJ, 459, 415 [arXiv:astro-ph/9508157]
- Wright, E. L. 2006, arXiv:astro-ph/0603075
- Yu, H., Ratra, B., & Wang, F.-Y. 2018, ApJ, 856, 3 [arXiv:1711.03437]
- Yu, H., & Wang, F. Y. 2016, ApJ, 828, 85 [arXiv:1605.02483]
- Zaldarriaga, M., Seljak, U., & Bertschinger, E. 1998, ApJ, 494, 491 [arXiv:astro-ph/9704265]
- Zhang, X., et al. 2017, Res. Astron. Astrophys., 17, 6 [arXiv:1703.08293]
- Zhao, G.-B., et al. 2007, Phys. Lett. B, 648, 8 [arXiv:astro-ph/0612728]
- Zhao, G.-B., Raveri, M., Pogosian, L., et al. 2017, Nat. Astron., 1, 627 [arXiv:1701.08165]